Creep behavior of a dispersion-strengthened Cu–Ti–Al alloy obtained by reaction milling

Rodrigo G. Espinoza[a,*], Rodrigo H. Palma[b], Aquiles O. Sepúlveda[b], Alejandro Zúñiga[b]

[a] *Departamento de Ciencia de los Materiales, FCFM, Universidad de Chile, Av. Tupper 2069, Santiago 8370451, Chile*
[b] *Departamento de Ingeniería Mecánica, FCFM, Universidad de Chile, Beauchef 850, 4° Piso, Santiago 8370448, Chile*

A B S T R A C T

Creep results of a dispersion-strengthened nominal-composition Cu-2.5 vol.%Ti-2.5 vol.%Al alloy, and the adjustment of those results to existing creep models, are presented. The alloy was prepared by reaction milling; its microstructural characterization by transmission electron microscopy had been recently reported elsewhere. Creep tests were here performed at 773, 973 and 1123 K, under loads that produced steady-state creep rates between 9×10^{-7} and $2 \times 10^{-4}\ s^{-1}$. Two deformation models, available in the literature, were considered: dislocation creep, where the strain rate is controlled by the dislocation-particle interaction within the grains, and diffusional creep, controlled by the interaction between grain-boundary dislocations and particles. In all creep experiments the alloy exhibited high values of the apparent stress exponent, as typical for dispersion-strengthened alloys. Through model adjustment, the operating creep mechanisms where determined: at 773 and 1123 K, creep is controlled by dislocation/particle interactions taking place in the matrix and in grain boundaries, respectively, while at the intermediate temperature of 973 K, controlling dislocation-particle interactions would occur both in the matrix and in grain boundaries.

Keywords:
Creep behavior
Copper alloys
Dispersion-strengthening
Reaction milling
Mechanical alloying

1. Introduction

Alloys exhibiting high mechanical strength together with high electrical and thermal conductivity at elevated temperatures are in increasing demand [1]. Due to its high electrical/thermal conductivity, copper is a most promising metal for all of these applications. Moreover, copper has the advantage of a low elastic modulus, which minimizes thermal stresses in actively cooled structures [2]. However, its strength must be increased in order to meet design requirements for high-temperature applications [3]. The high-temperature mechanical strength of metallic alloys can be increased by adding a small fraction (e.g., between 2 and 5 vol.%) of ceramic dispersoids. In contrast to solid-solution strengthening, the addition of elements to form insoluble particles has little effect on the electrical conductivity. To be most effective, these dispersoids must be thermodynamically stable, homogeneously distributed in the metal matrix and of nanometric size [1]. Reaction milling is a modern manufacturing process which uses mechanical alloying for the in-situ development of nanometric dispersoids in a metal matrix [4]. In reaction milling, elemental powders are milled under a controlled atmosphere and in a suitable milling medium so that one of the metals reacts with C, N, or O in order to form carbides, nitrides or oxides, respectively. Thus, dispersion-strengthened copper with improved mechanical behavior at high temperature [5,6] can be obtained.

On the other hand, upon adding ceramic dispersoids, the high-temperature strength of the material is mainly controlled by two deformation mechanisms: dislocation creep, where the strain rate is controlled by the dislocation-particle interaction within the grains [7], and diffusional creep, controlled by the interaction between grain-boundary dislocations and particles [8].

In a preceding paper [9], we described the processing and microstructural characterization of two dispersion-strengthened alloys of nominal-composition Cu-2.5 vol%TiC-2.5 vol% Al_2O_3, obtained by reaction milling and followed by extrusion. It was shown that one of the developed alloys, referred to as the H-20 alloy, presented a stable microstructure with Ti–Al–Fe nanodispersoids embedded in the Cu matrix. As demonstrated by transmission electron microscopy (TEM), at high temperature these dispersoids act as effective pinning sites for dislocations, thus controlling slip and grain growth. Regarding electrical conductivity, in the as-consolidated condition, at room temperature, such alloy presented an International Annealed Copper Standard (IACS) value of 59%.

This paper extends that earlier work to include additional experimental results and adjustment of models. First, results of

* Corresponding author. Tel.: +56 2 978 42 22; fax: +56 2 699 41 19.
E-mail address: roespino@ing.uchile.cl (R.G. Espinoza).

the creep behavior of a dispersion-strengthened Cu-2.5 vol%TiC-2.5 vol.%Al_2O_3 alloy prepared by reaction milling and extrusion (H20 alloy) are presented. Creep tests were performed at 773, 973 and 1123 K, under loads that produced steady-state creep rates between $\sim 9 \times 10^{-7}$ and $\sim 2 \times 10^{-4}\ s^{-1}$. These experimental results, taking into account the previously reported TEM microstructural characterization [9], are then analyzed within the framework of existing creep models [7,8], and the operating creep mechanisms are determined.

2. Antecedents of creep models based on particle-dislocation attraction

The creep behavior of polycrystalline dispersion-free alloys is properly expressed by the well-known Norton power law:

$$\dot{\varepsilon} = f(T)\sigma^n \tag{1}$$

where $f(T) = \exp(-Q/k_B T)$; $\dot{\varepsilon}$ is the strain rate; T is the temperature; σ is the strain; k_B is the Boltzmann constant; and n and Q are material constants. Thus, n is the stress exponent, stating the sensitivity of the strain rate, and Q is the pertinent creep activation energy.

Moreover, having in mind the same equation, the behavior of dispersion-strengthened (DS) materials is characterized by high values of the apparent stress exponent ($n = n_{ap}$) and apparent creep activation energy (Q_{ap}) [10], as opposed to dispersoid-free materials. Rösler and Arzt proposed a creep model for DS alloys (RA model) which is based on an attractive particle-dislocation interaction [7]. In this model, the creep-rate controlling process is the thermally-activated detachment of dislocations from the departure side of the particles contained within grains, and is given by:

$$\dot{\varepsilon} = \dot{\varepsilon}_0 exp\left(-\frac{Gb^2 r}{k_B T}\left[(1-k)\left(1-\frac{\sigma}{\sigma_d}\right)\right]^{3/2}\right) \quad \text{with } \dot{\varepsilon}_0 = \frac{6D_v L\rho}{b} \tag{2}$$

In Eq. (2), D_v is the bulk diffusion coefficient; L is the interparticle spacing; ρ is the dislocation density; b is the Burgers vector; G is the temperature-dependent shear modulus; and r is the particle (dispersoid or precipitate) radius. Additionally, the parameter k is the relaxation factor of the dislocation-line energy at the particle interface; and ρ_d is the detachment stress, which represents the attraction between dislocations and particles through the equation:

$$\sigma_d = \sigma_{Or}\sqrt{1-k^2} \tag{3}$$

where σ_{Or} is the Orowan stress. If the interface is coherent, then the dislocation is not attracted by the particle, and $k = 1$ as σ_d is zero. On the other hand, if the interface is semicoherent or incoherent, $k < 1$ as a non-zero σ_d stress needs to be applied to separate the dislocation from the particle.

The Orowan stress can be calculated as [8]:

$$\sigma_{Or} = 0.84\frac{M}{2\pi\sqrt{1-\nu}}\frac{Gb}{d_p}\sqrt{\frac{6f_v}{\pi}}\ln\left(\frac{d_p}{2b}\right) \tag{4}$$

where M is the Taylor factor, ν is the Poisson coefficient, f_v is the total volume fraction of dispersoids and d_p is the average particle diameter ($d_p = 2r$).

The RA model allows the calculation of the relaxation factor, k, and the detachment stress, σ_d, both related through Eq. (2), as follows [7].

$$k = 1 - \left(\frac{2k_B T}{3Gb^2 r}\frac{n_{ap}}{(1-(\sigma/\sigma_d))^{1/2}(\sigma/\sigma_d)}\right) \tag{5}$$

$$\frac{\sigma}{\sigma_d} = \left(\frac{3(Q_{ap}-Q_v)}{2RTn_{ap}(1-(\partial G/\partial T)(T/G))}+1\right)^{-1} \tag{6}$$

where Q_v is the activation energy for the vacancy movement in the matrix.

The above RA model has been successful in explaining the stress exponents observed in creep tests carried out at medium temperatures for DS alloys [7]. Nevertheless, in DS materials having ultra-fine grain sizes tested at elevated temperatures, the creep strain rate may be controlled by diffusional creep, and the RA model is unable to explain the high stress exponents observed in those cases. In this way, Rösler, Joos and Arzt (RJA) [8], motivated by experimental observations on creep in oxide dispersion-strengthened (ODS) Al alloys, proposed an alternative model (RJA model) for the case when the mechanism controlling the creep rate is the detachment of grain-boundary dislocations from precipitates situated at those grain boundaries.

Assuming that the dislocation bypass process is, as it is within the grains, controlled by thermally-activated dislocation detachment, a rate equation was derived, $\dot{\varepsilon}_{Dif}$ [8]:

$$\dot{\varepsilon}_{Dif} = \dot{\varepsilon}_{0,Dif} exp\left(-\frac{Gb_{gb}^2 r}{k_B T}\left[(1-k)\left(1-\frac{\sigma}{\sigma_d}\right)\right]^{3/2}\right),$$

$$\text{with } \dot{\varepsilon}_{0,Dif} = \frac{4D_{gb}L\rho_{gb}}{d_g b_{gb}} \tag{7}$$

where D_{gb} is the self-diffusion coefficient at the grain boundaries, ρ_{gb} is the dislocation density at the grain boundaries, b_{gb} is the Burgers vector of a grain-boundary dislocation, typically estimated as 0.5 to 0.3b [11], and d_g is the matrix grain size.

In a creep study of ultrafine-grained ODS copper prepared by cryomilling, Kudashov et al. [12] proposed the use of an effective diffusion coefficient, D_{eff}, in Eq. (7), instead of the standard grain-boundary diffusion coefficient D_{gb}. So, D_{eff} incorporates the simultaneous effect of volume diffusion (D_v) and pipe diffusion (D_c) on the dislocation movement:

$$D_{eff} = D_v + \frac{t\pi D_{gb}}{d_{gb}} + \rho_{gb}D_c \tag{8}$$

where t is the grain-boundary thickness.

3. Experimental procedure

A nominal-composition Cu-2.5vol.%TiC-2.5vol.%Al_2O_3 alloy was produced by reaction milling, from elemental powders of the pertinent metallic elements (Cu, Ti and Al). Spheroidal powders of atomized Cu (90 wt. % under 45 μm), Ti (<45 μm) and Al (80 wt.% under 45 μm) were employed. The milling process was carried out in a Szegvari-type attritor, with a ball to powder weight ratio (BPR) of 10:1 and a rotational speed of 500 rpm, according to a two-step procedure. The first step consisted in milling Cu and Al powders for 1 h under a nitrogen atmosphere using hexane (C_6H_{14}) as the milling medium, followed by powder drying, and addition of Ti elemental powders. In the second step, this mixture was milled for 20 h under a nitrogen atmosphere using hexane as the milling medium. The O and C necessary for the in situ formation of nanodispersoids was provided by the reduction of superficial copper oxides and the liquid hexane medium, respectively. The resulting aggregates were encapsulated at low vacuum and then consolidated by hot extrusion at 1023 K, using an extrusion ratio of 10:1. Other processing details are described elsewhere [9].

Cylindrical specimens 6.5 mm in diameter and 9.8 mm in length were machined from as-extruded bars, with the axis parallel to the extrusion direction. Room-temperature compression tests were

carried out to determine yield strength values, data which were subsequently used to estimate the σ_{Or} values. Constant-stress compression creep tests were performed in a TT-DM Instron machine, equipped with a high-temperature compression facility apparatus designed and built in house. The test temperature was monitored by a thermocouple located at the lower plate of the compression stage near the specimen. The load was monitored by the load cell of the Instron machine, while the displacement was measured with a DFG5 Solartron extensometer, attached to the external machine linkage. Both data were acquired using a PCL711B Advantech board, and logged as a function of time onto a desktop computer. Finally, a computer software permitted the control of the applied stress on the sample. Tests were performed at 773, 973 and 1123 K, under loads that produced steady-state creep rates between $\sim 9 \times 10^{-7}$ and $\sim 2 \times 10^{-4}\ s^{-1}$. The temperature during the creep tests was stabilized within 1 K. Prior to creep testing, Vickers microhardness (100 g) measurements were performed on each specimen, to verify the homogeneity of the material. Transmission electron microscopy (TEM) observations were performed with the main purpose of measuring the particle volume fraction in the H-20 alloy. A Tecnai ST F20 (FEI) microscope was employed. Observed specimen thickness was determined on an across-the-thickness single grain, using a convergent-beam electron diffraction pattern under a two-beam condition with the $g = (2\,2\,2)$ reflection excited. Crystal thickness was measured based on the extinction lines present within the $(2\,2\,2)$ diffraction disc, using the lineal regression method described by Williams and Carter [13]. As particles where spherical, their volume was determined from particle radius measurements.

4. Results

4.1. Initial materials

The characterization and microstructural description of the H-20 alloy used in the present creep tests has been reported elsewhere [9]. Briefly, the material exhibited a stable microstructure with nanodispersoids homogeneously distributed both at the grain boundaries and within the grains. TEM observations showed that these dispersoids were very efficient in retaining the grain size obtained after hot-extrusion consolidation. The dispersoids were identified mainly as Al_2O_3 and Ti–Al–Fe particles. Material observations after annealing at 1123 K for 1 h, and after compression test at 1123 K, also showed the dispersoids pinning effect over dislocation gliding and grain growth. The mean grain and dispersoid sizes were $d_{gi} = 140$ nm and $d_{pi} = 6.1$ nm, respectively.

Complementary TEM observations were performed as part of this paper to determine an experimental value of dispersoid volume fraction within grains. Thus, a measured fraction, f_m, of 0.0265 was obtained for the H-20 alloy.

The mean interparticle spacing L was estimated using the following well known stereological relation [14], considering $d_p = 6.1$ nm and $f_v = f_m = 0.0265$ as above indicated:

$$L = \frac{d_p}{2}\sqrt{\frac{2\pi}{3f_v}} \tag{9}$$

Thus, a value $L = 27$ nm was obtained. The above microstructural parameters are summarized in the first lines of Table 1.

On the other hand, under the assumption that all the Al and Ti detected in the alloy chemical analysis [9] reacts forming Al_2O_3 and TiC particles, a total volume fraction for these two dispersed phases $f_0 = 0.049$ is obtained. The difference between this value and f_m is here associated to the precipitation of dispersoids in grain boundaries.

Table 1
Microstructural and mechanical behavior parameters of H20 extruded alloy

Initial grain size, d_{gi} [a] [9]	140 nm
Final grain size, d_{gf} [b] [9]	156 nm
Initial dispersoid diameter, d_{pi} [a] [9]	6.1 nm
Dispersoid diameter, d_{pf} [b] [9]	6.8 nm
Dispersoids volume fraction (calculated), f_0	0.0490
Dispersoids volume fraction (measured), f_m	0.0265
Interparticle spacing (calculated from Eq. (8) using d_{pi}), L	27 nm
Interparticle spacing (calculated from Eq. (8) using d_{pf}), L	31 nm
Orowan stress, σ_{Or}	
from Rösler equation	498 MPa
from Besterci equation	278 MPa
Room-temperature yield strength, σ_Y (measured)	745 MPa

[a] Values measured in as-extruded material.
[b] Values measured in as-extruded and tested in creep at 1123 K material.

4.2. Orowan stress

The room-temperature Orowan stress for the material was calculated using Eq. (4), the d_{pi} and L structural parameters of Table 1, and the following values: $M = 3.07$ for fcc materials [15], and $G = 42.1$ GPa [16] and $b = 0.256$ nm for copper. The resulting σ_{Or} value calculated from the Rösler equation, 498 MPa, is shown in Table 1. On the other hand, the Orowan stress was also calculated assuming a linear contribution of the reinforcement mechanism to the yield strength, as it were proposed by Besterci et al. [17]:

$$\sigma_Y = \sigma_{Or} + \sigma_D + \sigma_0 + \sigma_{HP} \tag{10}$$

where σ_Y is the measured room-temperature yield strength, 745 MPa; σ_D is the contribution of dislocation strengthening, which was calculated as [17]:

$$\sigma_D = 2\alpha G b\sqrt{\rho} \tag{11}$$

where $\alpha = 0.2$ is the strength coefficient of the dislocation network [17], and ρ is the dislocation density, which for the alloy under study can be estimated as $1 \times 10^{13}\ m^{-2}$ [18]. With these values, σ_D is 14 MPa. Moreover, $\sigma_0 = 26$ MPa is the Peierls-Nabarro strengthening for Cu [19], $\sigma_{HP} = k_{HP} d_g^{-1/2}$ is the contribution according to Hall-Petch reinforcement (for Cu, $k_{HP} = 0.16\ MPa\sqrt{m}$ [19]. Considering a grain size of 140 nm (see Table 1), $\sigma_{HP} = 428$ MPa is obtained. With these values, Eq. (10) can be written as:

$$\sigma_Y = \sigma_{Or} + 14\ MPa + 26\ MPa + 428\ MPa = 745\ MPa \tag{12}$$

Finally, subtracting the numerical values from σ_Y in Eq. (12), σ_{Or} from the Besterci equation gives 278 MPa, as indicated in Table 1. The values of the individual hardening contributions show that the grain boundaries provide the largest contribution. They contribute roughly to 60% of σ_Y, whereas the remainder is caused directly by the nanoparticles through the Orowan mechanism. Similar proportional values were observed by Kudashov et al. [12].

The overestimation of the Orowan stress calculated from Eq. (4) in comparison with the value obtained from the Besterci equation (Eq. (10)), could be explained by the uncertainty in the assumptions and parameters used in the calculations. Moreover, dispersoids precipitated at grain boundaries would not participate in the Orowan reinforcement mechanism, diminishing the effective volume fraction into the grains, and increasing the interparticle distance between dispersoids. Similar disagreements between the theoretical and experimental values of σ_{Or} were reported by Nagorka et al. [20].

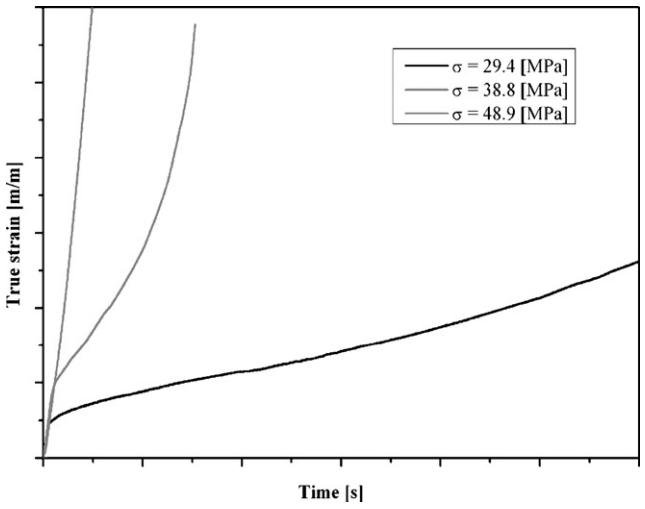

Fig. 1. Representative strain–time plots for creep at 1123 K and various applied stress levels.

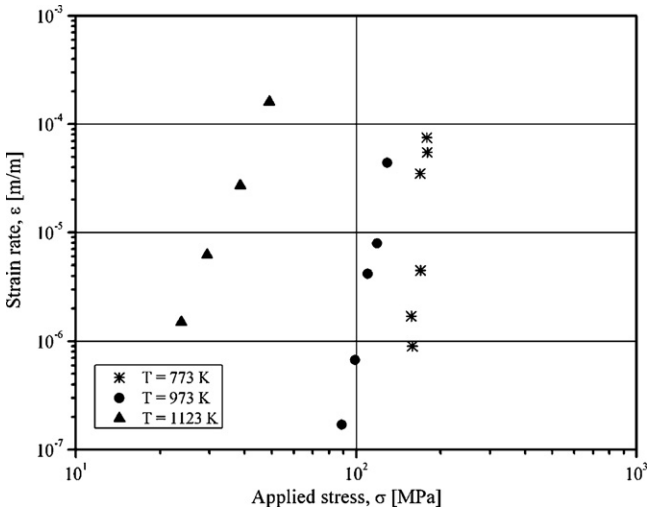

Fig. 2. Strain rate versus applied stress creep results.

4.3. Creep results

Constant-stress creep tests of the alloy under study were here performed at temperatures of 773, 973 and 1123 K. The material exhibited strain versus time curves with shapes similar to those presented in Fig. 1, which correspond to 1123 K. The applied stress and the resulting strain rate for the secondary creep stage of these curves, at the temperatures considered, are shown on a log–log plot in Fig. 2. It can be seen in that figure that, for each temperature, the experimental data can be described by a linear relationship.

Based on the microstructural observations presented elsewhere [9], where dispersoids observed by TEM efficiently limited the grain growth, the RA model of creep controlled by dislocation detachment appears to be applicable to the present creep results [7]. In order to analyze the data according to this theory, it is necessary to experimentally determine values for the apparent stress exponent, n_{ap}, and the corresponding apparent energy for creep, Q_{ap}. The values for n_{ap} were directly obtained by linear regression of the log–log plot of Fig. 2 and summarized in Table 2. These values present similar behavior to that of n_{ap} results reported by other authors for ODS copper with different dispersoids (see Table 2). The values reported by Frost and Ashby [16] for pure copper are also included.

It is observed that at low test temperatures (~773 K) the values for n_{ap} obtained in the present work and different ODS copper alloys are higher than 20, similar to other dispersion-strengthened alloys [20]. These values typically decrease with an increase in temperature. In the case of dislocation creep, n_{ap} has values between 3 and 5 (4.8 for pure copper), while for diffusional creep, the apparent stress exponent shows values between 1 and 2.

The apparent activation energy was calculated at constant σ/G based on the expression [10]:

$$Q_{ap} = \left(\frac{\partial \ln \dot{\varepsilon}}{\partial T}\right)_{\sigma/G} RT^2 \tag{13}$$

where R corresponds to the gas constant. To use Eq. (13), the temperature-dependent G modulus data given by Frost and Ashby [16] presented in Eq. (14) were used.

$$G = G_0\left(1 - 0.54\frac{T - 300}{T_F}\right) \tag{14}$$

The three Q_{ap} values thus obtained are shown in Table 2, and are higher than those reported elsewhere for pure copper under power law creep [16]. It is known that the energies observed in dispersion-strengthened materials attain values that are greater than all the activation energies for the various diffusion mechanisms [10]. Moreover, significantly different Q_{ap} values were obtained for the present alloy at each of the three temperatures studied, indicating that different creep mechanisms were active at different temperatures.

It has been shown that the microstructure of the Cu–Al–Ti alloy, as consequence of its fabrication route, exhibits a fine grain size. However, the Q_{ap} energies for the alloy under study are much higher than the activation energies corresponding to lattice self-diffusion in copper (Q_{SD} = 197.0 kJ/mol [16]), dislocation core diffusion (Q_{DC} = 147.4 kJ/mol [21]), and grain-boundary diffusion (Q_{GB} = 133.9 kJ/mol [22]). Then, from this discussion it is not evident which diffusion mechanism controls the thermally activated creep process. Nevertheless, lattice self-diffusion, dislocation core

Table 2
Values of n_{ap} and Q_{ap} for the present and other ODS Cu based alloys, at various temperatures

Alloy (nominal vol.% of dispersoids)	Test temperature (K)	n_{ap}	Q_{ap} (kJ/mol)
Cu – 2.5 Al_2O_3 – 2.5 TiC (present work)	773	31.2	357.1
	973	14.7	572.2
	1123	6.3	770.7
Cu [16]	923 – 973	4.8	197.0
Cu – 3 TiC [5]	773	>100	Not reported
Cu – 0.7 Al_2O_3 (GlidCop Al-15) [10]	748–773	21.8–19.4	257.6
	973–998	10.2–10.6	248.9
Cu – 1 Y_2O_3 [20]	923–973	7.1–8.8	530.0
Cu – 1 ZrO_2 [20]	923–973	10.1–12.2	486.0–535.0
Cu – 3 Y_2O_3 [12]	773–973	22–9	Not reported

diffusion and grain-boundary diffusion will be analyzed below within the framework of the thermally-activated detachment model.

4.4. Relaxation factor and dislocation-particle detachment stress

From the Rösler–Arzt equations for strain-rate control Eq. (2) [7], the necessary stress to detach a dislocation retained by a matrix dispersoids (σ_d), and the parameter representing the energy line relaxation of a dislocation retained by a dispersoid-dislocation interface (k), can be derived (Eqs. (5) and (6)). Thus, the ratio between the applied stress and the detachment stress (σ/σ_d) was first calculated for each vacancy transport mechanism, using Eq. (6); then, employing such ratios, the interaction parameters k were calculated for each considered temperature using Eq. (5).

The Orowan stress was calculated using Eq. (4), considering a value of the volume fraction $f_v = f_m$, of 0.0265 (see Table 1). The resulting k and σ_d values are summarized in Table 3.

As it can be seen in Table 3, the obtained k values are within a rather narrow range ($0.75 < k < 0.80$) around the lower limit of the range indicated by Rösler–Arzt [7] for a variety of interaction intensities ($0.77 < k < 1.0$). Incidentally, for alumina dispersoids in the GlidCop Al-15 alloy, Broyles et al. [10] found values close to 0.9, which represent a moderately strong interaction, and an interface matrix-dispersoid partially coherent. On the other hand, Sauer et al. [5] determined values of $k = 0.75$ for Cu alloys with TiC dispersoids.

4.5. Application of the Rösler–Arzt model to creep behavior

The k and σ_d values of Table 3 can be used to apply the RA model [7], see Eq. (2), to the creep behavior of the alloy under study. This model considers the interaction of dislocations with fine particles dispersed in the matrix as the controlling creep mechanism. The model adjustment should indicate us whether such interaction takes place, and the vacancy diffusion mechanism controlling the strain rate for the experimental results.

Regarding the application of Eq. (2), firstly, D_v can be calculated as $D_V = D_0 \exp(-Q/RT)$, with D_0 being the pre-exponential value for the pertinent diffusion mechanism, and R the gas constant. In Table 4, D_0 and Q values for each vacancy diffusion mechanism are presented. Moreover, for the dislocation density, as for the preceding Orowan stress calculations, a value of $\rho = 1 \times 10^{13}\ m^{-2}$ [18] was employed.

The calculated curves using the RA model were drawn and compared with the actual creep tests data, for each of the diffusion mechanisms considered, see Fig. 3. It is there observed that the calculated curves do not fit properly in the case of dislocation and grain-boundary diffusion, see Fig. 3b and c; thus, these two mechanisms can be discarded. Moreover, at 1123 K (Fig. 3a), the calculated curves are again far away from the experimental results, indicating that for that temperature the RA model does not apply for any of the diffusion mechanisms considered. On the other hand, as seen in Fig. 3a, the calculated curves adequately fit the creep data at 773 and 973 K, when bulk diffusion is considered as the main transport mechanism. This suggests that, for these temperatures, the strain-rate controlling mechanism is dislocation pinning by dispersoids within the grain, where the predominant transport mechanism of vacancies is the self-diffusion, with k close to 0.80 at both temperatures (detachment-controlled matrix creep).

The variations observed for n_{ap} at different temperatures is characteristic for DS alloys reinforced by nanoparticles, where a region of high apparent stress exponent is observed. Aluminum alloys studied by Rösler et al. [8] showed high stress-sensibility ($n_{ap} > 50$) at intermediate strain rates ($10^7\ m^{-2} \dot{\varepsilon}/D < 10^{11}\ m^{-2}$, where D is

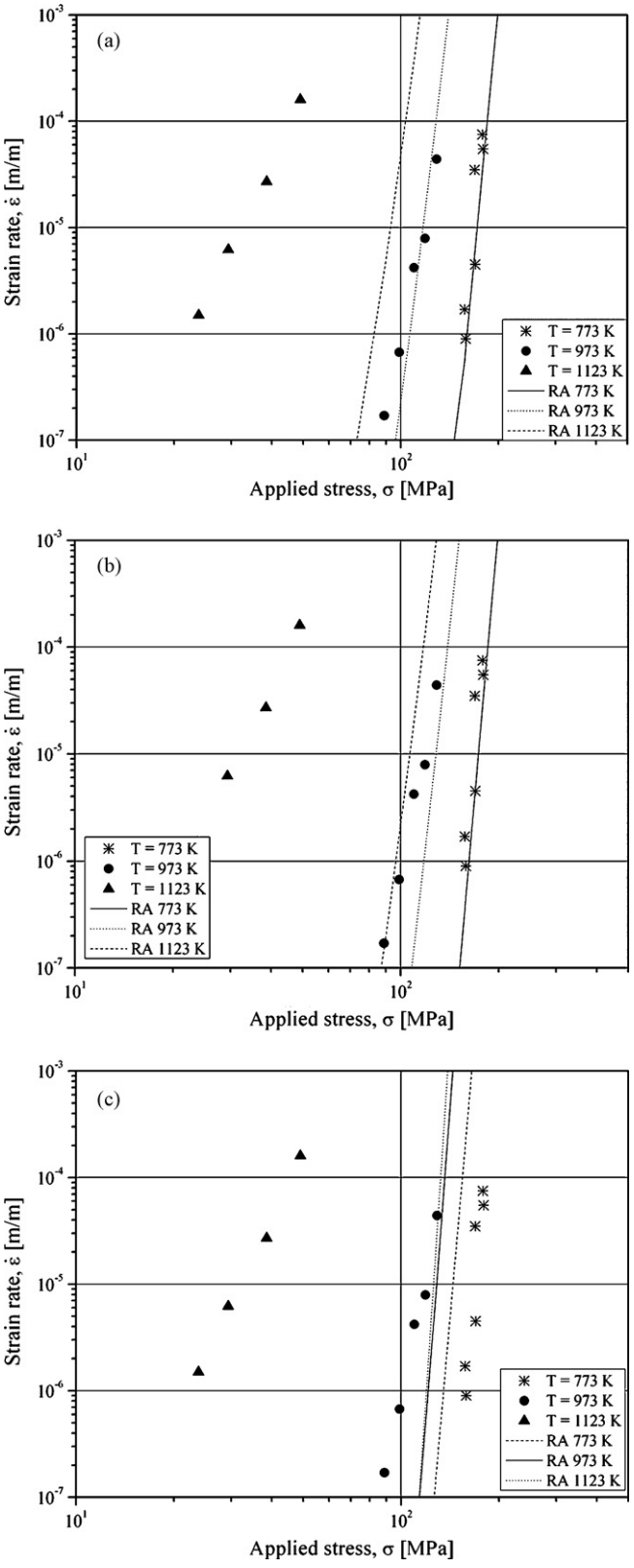

Fig. 3. Experimental data and Rösler–Arzt model curves for each diffusion mechanism: (a) Self-diffusion; (b) dislocation core; (c) grain boundaries.

Table 3
Calculated parameters for the Rösler–Arzt model

Test temperature (K)	n_{ap}	Q_{ap} (kJ/mol)	Transport mechanism					
			Self-diffusion		Dislocation core		Grain boundaries	
			k	σ_d (MPa)	k	σ_d (MPa)	k	σ_d (MPa)
773	31.2	357.1	0.80	241	0.79	246	0.79	247
973	14.7	572.2	0.79	224	0.77	229	0.77	231
1123	6.3	770.7	0.76	215	0.75	220	0.75	221

the self-diffusion coefficient). Based on TEM images taken after creep deformation, Rösler et al. proposed that the rate controlling deformation mechanism is the interaction of single dislocations with dispersoid particles. At high creep rates ($\dot{\varepsilon}/D > 10^{11}\,m^{-2}$) the stress exponent decreases, which is expected because otherwise the creep rate of the dispersion-strengthened material would eventually exceed that of the dispersion-free matrix material at high stresses. Consequently, the stress exponent of the dispersion-strengthened material may stay relatively high ($n \gg 3$–5), although the deformation mechanism becomes "matrix-like". Rösler et al., in an ODS aluminum alloy, suggested that the observed decrease of the stress exponent values with the test temperature could be attributed to diffusional creep, which would be controlled by an interface interaction. Those authors assumed that the generation and annihilation of vacancies requires the slip of "grain-boundary" dislocations, which have to overcome dispersoids situated at the grain boundaries. The application of the "new" model (RJA model), represented by Eq. (7), to the present creep results is shown in Fig. 4, where the calculated lines and the experimental creep data points are presented.

Fig. 4 presents a good agreement between the model of Eq. (7) with the creep results at 1123 K, using a grain-boundary dislocation density, ρ_{bg}, of $10^{-5}\sigma/2Gb$ [8], and a b_{bg} value of 0.55b. In this case, a dispersoid volume fraction of 0.265, f_m, and 0.225, $f_0 - f_m$, within grains and at grain boundaries were used, respectively. Dispersoid diameters of 6.8 nm, d_{pf}, corresponding to a mean interparticle spacing L of 31 nm, and a grain-boundary diameter of 156 nm, were also used (see Table 1). The selection of these values is justified by the microstructural observations of the material creep tested at 1123 K, where a light increase of the grain-boundary size and dispersoid diameter was observed [9]. The effective diffusion coefficient proposed by Kudashov et al. was used (D_{eff} in Eq. (8)), with a grain-boundary thickness (t) of 1 nm.

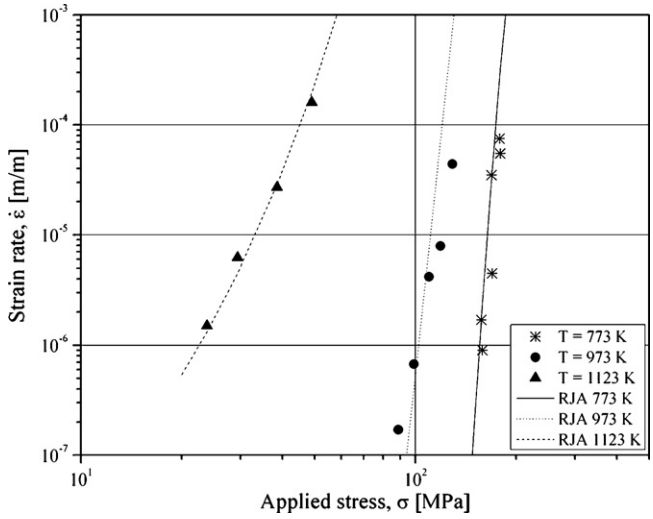

Fig. 4. Application of Eq. (7) from Rösler–Joos–Arzt model to the present creep results.

For the application of Eq. (7), the k factor is manipulated as a free parameter, different to the k values used in the calculations of the first model. For the adjustment at 1123 K this factor was estimated as $k = 0.75$, which is closer to the value presented in Table 3 for grain-boundary transport mechanism. Following the same procedure just described, it is possible to properly fit model curves to the experimental results for 773 and 973 K. However, this gives rise to k values of 0.50 and 0.55, respectively, which are significatively below the lower limit of 0.77 established by Rösler et al. in their original model [7].

5. Discussion

The experimental creep results presented in this work for a copper DS alloy, together with the microstructural evidence previously reported [9], suggest that the acting creep controlling mechanisms can be related to the interaction between dislocations and dispersoids, according to RA and RJA models. The adjustment of the RA model, represented by Eq. (2), shows that the best fit for the results at 773 and 973 K (Fig. 5) corresponds to a transport mechanism of self-diffusion. The agreement between the experimental and modeling n_{ap} exponents is good for 773 K (31.2 against 32.7), but rather poor for 973 K (14.7 against 23.6). On the other hand, for 1123 K, a proper adjustment is obtained with the RJA model, represented by Eq. (7), with an acceptable agreement between experimental and

Table 4
Pre-exponential factors, D_0, and activation energies, Q, for different diffusion mechanisms, as reported in literature

Diffusion mechanism	D_0 (m^2/s)	$Q_{activation}$ (kJ/mol)
Self-diffusion [23]	2.0×10^{-4}	197.0
Dislocations [23]	2.4×10^{-7}	147.4
Grain boundaries [16]	2.5×10^{-5}	133.9

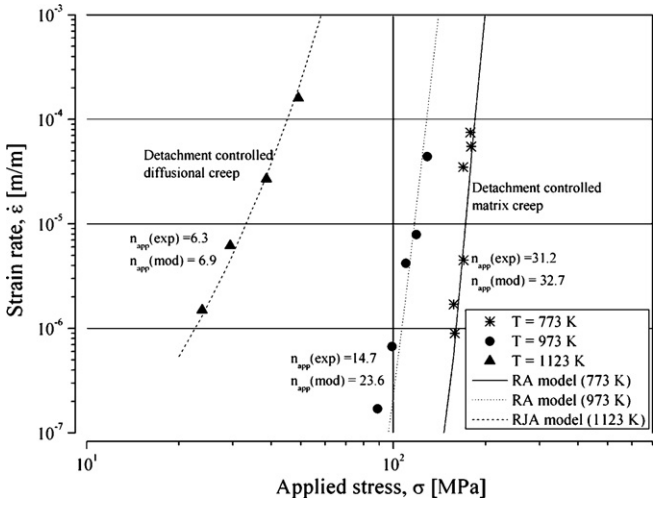

Fig. 5. Comparison between Rösler models and our experimental creep tests values.

Table 5
Creep control mechanisms in dispersion-strengthened Cu-based alloys as reported in this paper and in literature

Alloy (nominal vol.% of dispersoids)	Test temperature (K)	Creep control mechanism
Cu – 2.5 Al_2O_3 – 2.5 TiC (present work)	773	Detachment controlled matrix creep
	973	Detachment controlled matrix creep, possible mixed mechanism
	1123	Detachment controlled diffusional creep
Cu – 0.7 Al_2O_3 (GlidCop Al-15) [10]	748 – 773	Detachment controlled matrix creep, possible mixed mechanism
	973 – 998	
Cu – 3 TiC [5]	773	Detachment controlled dislocation (matrix) creep
Cu – 1 Y_2O_3 [20]	923 – 973	Detachment controlled diffusional creep at low stress.
Cu – 1 ZrO_2 [20]	923 – 973	Detachment controlled matrix creep at high stress
Cu – 3 Y_2O_3 [12]	773 – 973	Detachment controlled diffusional creep

modeling n_{ap} parameters (6.3 against 6.9). Thus, for 773 and 1123 K the creep-rate control can be associated to dislocation detachment from particles, within the matrix (matrix creep) and within grain boundaries (diffusional creep), respectively. Additionally, for 973 K, a mixed strain rate control, in terms of interactions both within the matrix and grain boundaries, is possible, a behavior which has been previously reported for other alloys [10,12,20].

The values obtained for the relaxation factor, k, are in the 0.75-0.80 range, which represents a high relaxation energy associated to the dislocation detachment from the nanometric dispersoids and, accordingly, a high resistance to such detachment. As temperature increases, the values of the n_{ap} exponents decrease. In all cases, these values are clearly above those corresponding to pure copper and follow the tendency observed in other DS alloys (see Table 2).

Creep-rate controlling mechanism informed by other authors for various dispersion-strengthened Cu-based alloys, deduced under the frame of the RA and RJA models, as well as the results of this paper, are presented in Table 5. This summary shows that in the considered creep results, high k values, corresponding to a strong particle-dislocation interaction, were obtained. On the other hand, when the present creep results are compared with those of other DS alloys for the same type of dispersoids (Cu – 0.7vol.% Al_2O_3 [10] and Cu – 3 vol.% TiC [5]), it is verified that a detachment-controlled matrix creep has been consistently determined at 773 K. A possible mixed mechanism is also proposed by Broyles et al. for the Cu – 0.7 vol.% Al_2O_3 creep results near 973 K.

In our TEM characterization of the Cu–Ti–Al alloy, evidence of the presence of nanometric particles in grain boundaries was presented; more recently, we verified that they correspond to TiC particles. Besides, the RJA model assumes the attachment of grain-boundary dislocations on particles located at grain boundaries. According to our best knowledge, no observations have been reported on direct support of that assumption. It should be noted that a TEM verification of such particle-dislocation interaction is somewhat hard due to the specific characteristics of the object to be observed, especially in the case of high-angle boundaries. The grain-boundary dislocation detachment is suggested by the evidence of particles in grain boundaries and the good adjustment of the RA and RJA models with experimental creep results [12,20].

The use of an effective diffusion coefficient, D_{eff} (see Eq. (8)), as a modification of the original RJA model proposed by Kudashov et al. [12] permitted us to obtain a better fit with the creep results at 1123 K. With such modification, different possible transport mechanisms that may act at high temperature can be considered.

Finally, the high stability presented by the nanometric dispersoids formed in the Cu–Ti–Al alloy [9], in a range of normalized temperatures between 0.6 and 0.85 T/T_M (T_M = melting temperature of Cu), suggests the applicability of this material in high-temperature applications, when elevated mechanical resistance and good electrical conductivity are important.

6. Conclusions

The present Cu–Ti–Al alloy exhibited, under creep tests performed at 773, 973 and 1123 K, high values of the apparent stress exponent (n_{ap}(exp) = 31, 15 and 6, respectively), as typical for dispersion-strengthened alloys.

The application of the RA and RJA models to the Cu–Al–Ti creep results, leads to conclude that at 773 and 1123, creep is controlled by dislocation/particle interactions taking place in the matrix and in grain boundaries, respectively, while at the intermediate temperature of 973 K, controlling dislocation/particle interactions would occur both in the matrix and in grain boundaries. For all temperatures, the obtained values for the relaxation factor are in the range 0.75–0.80, corresponding to a high resistance of dislocation detachment from particles.

Acknowledgements

The authors acknowledge the financial support of project Fondecyt No. 1011024. R. Espinoza acknowledges Conicyt for the scholarship and financial support for his Doctoral Thesis.

References

[1] J.R. Groza, J.C. Gibeling, Mater. Sci. Eng. A171 (1993) 115–125.
[2] I. Anzel, A.C. Kneissl, L. Kosec, Z. Metalkd. 90 (1999) 621–635.
[3] R. Palma, A. Sepúlveda, R. Espinoza, R. Montiglio, J. Mater. Proc. Technol. 169-1 (2005) 62–66.
[4] L. Lü, M.O. Lai, Mechanical Alloying, Kluwer Academics Publishers, Massachusetts, EEUU, 1998.
[5] C. Sauer, T. Webgärber, G. Dehm, J. Mayer, W. Püsche, B. Kieback, Z. Metallkd. 89 (2) (1998) 119–125.
[6] R. Palma, A. Sepúlveda, A. Zúñiga, R. Pérez., Molienda reactiva de aleaciones Cu–Ti–C, Anales de las Jornadas SAM-CONAMET-AAS 2001, Posadas, Argentina, Septiembre (2001) 317–324.
[7] J. Rösler, E. Arzt, Acta Metall. Mater. 38 (1990) 671–683.
[8] J. Rösler, R. Joos, E. Arzt, Metall. Trans. 23A (1992) 1251–1539.
[9] R.A. Espinoza, R.H. Palma, A.O. Sepúlveda, V. Fuenzalida, G. Solórzano, A. Craievich, D. Smith, T. Fujita, M. López, Mater. Sci. Eng. A 454–455 (2007) 183–193.
[10] S.E. Broyles, K.R. Anderson, J.R. Groza, J.C. Gibeling, Metall. Trans. A 27A (1996) 1217–1227.
[11] E. Arzt, M.F. Ashby, R.A. Verrall, Acta Metall. 31 (1983) 1977–1989.
[12] D.V. Kudashov, H. Baum, U. Martin, M. Heilmaier, H. Oettel, Mater. Sci. Eng. A 387–389 (2004) 639–642.
[13] D.B. Williams, C.B. Carter, Transmission Electron Microscopy, Plenum Press, New York, 1996, pp. 321–323.
[14] G. Le Roy, J.D. Embury, G. Edwards, M.F. Ashby, Acta Metall. 29 (8) (1981) 1509–1522.
[15] G.I. Taylor, J. Inst. Met. 62 (1938) 307.
[16] H.J. Frost, M.F. Ashby, The Plasticity and Creep of Metals and Ceramics, Pergamon Press, Oxford, 1982, p. 21.
[17] M. Besterci, Scripta Met. et Mater. 30-9 (1994) 1145–1150.
[18] G.J. Lloyd, J.W. Martin, Mater. Sci. Eng. 46 (1980) 1–13.
[19] K.R. Anderson, J.R. Groza, Met. Mater. Trans. A 32 (2001) 1211–1223.
[20] M.S. Nagorka, G.E. Lucas, C.G. Levi, Metall. Mater. Trans. A 26 (1995) 873–881.
[21] R.W. Ballufi, Phys. Status Solidi 42 (1970) 11–34.
[22] W.B. Beeré, G.W. Greenwood, Met. Sci. J 5 (1971) 107–113.
[23] K. Kuchařová, S. Zhu, J.J. Čadek, Mater. Sci. Eng. A 348 (2003) 170–179.